Crystal Growth Technology

HANS J. SCHEEL
SCHEEL CONSULTING, Groenstrasse, CH-3803 Beatenberg BE, Switzerland
hans.scheel@bluewin.ch

TSUGUO FUKUDA
Institute of Multidisciplinary Research for Advanced Materials, Tohoku University, Sendai 980-8577, Japan
t-fukuda@tagen.tohoku.ac.jp

WILEY

4 Theoretical and Experimental Solutions of the Striation Problem

HANS J. SCHEEL
SCHEEL CONSULTING, Sonnenhof 13, CH-8808 Pfaeffikon, Switzerland

ABSTRACT

Striations are growth-induced inhomogeneities that hamper the applications of solid-solution crystals and of doped crystals in numerous technologies. Thus the optimized performance of solid solutions often can not be exploited. It is commonly assumed that striations are caused by convective instabilities so that reduced convection by microgravity or by damping magnetic fields was and is widely attempted to reduce inhomogeneities.

In this chapter it will be shown that temperature fluctuations at the growth interface cause striations, and that hydrodynamic fluctuations in a quasi-isothermal growth system do not cause striations. The theoretically derived conditions were experimentally established and allowed the growth of striation-free crystals of $KTa_{1-x}Nb_xO_3$ 'KTN' solid solutions for the first time.

Hydrodynamic variations from the accelerated crucible rotation technique (ACRT) did not cause striations as long as the temperature was controlled within 0.03 °C at 1200 °C growth temperature. Alternative approaches to solve the segregation and striation problems are discussed as well.

4.1 INTRODUCTION

Solid solutions or mixed crystals are special crystals or alloys in which one or more lattice sites of the structure are occupied by two or more types of atoms, ions or molecules. By varying the concentration of the constituents, the physical or chemical properties of solid solutions can be optimized for specific applications, so that solid solutions play an increasing role in research and technology. One example are III-V semiconductors where the bandgap and thus emission and absorption wavelengths can be adjusted, along with the lattice constant to match the available substrates for epitaxial growth, for optical communication systems. Another example are III-V compounds for photovoltaic devices where

Crystal Growth Technology, Edited by H. J. Scheel and T. Fukuda
 ISBN: 0-471-49059-8

the composition can be adjusted to optimize the solar-cell efficiency and to maximize radiation resistance (Loo *et al.* 1980). In certain cases, properties and effects may be obtained in solid solutions that are not observed in the constituents: The phase transition temperature and the related anomaly of a high dielectric constant may be shifted to the application temperature for electro-optic, nonlinear-optic and acousto-optic applications (Chen *et al.* 1966, Scheel and Günter 1985). The hardening effect of solid solutions is often used to improve the mechanical properties (Nabarro 1975).

The statistical distribution of species in a given lattice site normally is at random, but can deviate in the direction of ordering (with the extreme case of a superlattice) or in the direction of clustering (with the extreme case of immiscibility or phase separation) as it was shown by Laves 1944. This site distribution has an impact on the physical properties and can be controlled to some extent in metallic alloys, with their high diffusivities, by preparation or annealing conditions. However, in oxide systems with low diffusivities, the control of the distribution of species on lattice sites during crystal growth experiments has not been reported and will not be considered here.

In this chapter the bulk fluctuations of concentration will be treated with respect to the application-dependent homogeneity requirements, the types of inhomogeneities and their origin, and how inhomogeneities can be reduced or completely suppressed. There is a strong tendency for fluctuations of the growth conditions causing concentration fluctuations along the growth direction known as striations or growth bands. The suppression of striations is an old problem in crystal-growth technology, so that several authors had described striations as an 'intrinsic', 'inherent' or 'unavoidable' phenomenon in crystal growth, see Rytz and Scheel 1982, Scheel and Günter 1985.

Based on the segregation analyses for melt growth by Burton *et al.* (1953) and for growth from diluted solutions by Van Erk 1982, the role of hydrodynamics will be discussed, and the experimental conditions for growth of striation-free crystals derived. This theoretical result will be confirmed by the growth of quasi striation-free crystals of solid solutions. Finally, alternative approaches to reduce or eliminate striations are discussed, also novel approaches that require to be tested.

4.2 ORIGIN AND DEFINITIONS OF STRIATIONS

Nearly all crystals have inhomogeneities and growth bands called striations. Early observations of striations in semiconductor crystals have been reported by Goss *et al.* (1956) and by Bardsley *et al.* (1962) and for CaF_2 by Wilcox and Fullmer (1965). Hurle (1966) has shown for semiconductor crystals and Cockayne and Gates (1967) for Czochralski-grown oxide and fluoride crystals, that striations are caused by temperature fluctuations that may be correlated with thermal unsymmetry or with convective oscillations when a critical Rayleigh number is surpassed.

Many compounds like GaAs and $LiNbO_3$ are not line compounds, but have an existence range, that is they have a certain degree of solid solubility with one or both of the constituents. This causes a difference of the congruent melting composition from the stoichiometric composition. Therefore the grown crystals show variations of composition, often in the form of striations, depending on the exact growth conditions (melt composition and growth temperature and their fluctuations). This topic is discussed by Miyazawa in this volume for oxides and by Wenzl *et al.* (1993) for GaAs and compound semiconductors.

Also, melt-grown elements like silicon and line compounds like Al_2O_3 show striations due to impurities, in the case of silicon–oxygen striations from partial dissolution of the SiO_2 crucible. Very pronounced striations are often found in doped crystals (semiconductors, lasers) and in crystals of solid solutions.

The homogeneity requirements depend on the material and on the application. Examples of the maximum composition (X) variations $\Delta X/X$ are given in Table 4.1.

Corresponding to these tolerance limits, analytical methods are to be applied or developed in order to assist in the achievement of 'striation-free' crystals. In addition to the well-established methods to visualize striations, Donecker *et al.* (1996) developed a colorful optical diffraction method to visualize striations and demonstrated it with oxide, doped InP and $Si_{1-x}Ge_x$ crystals.

It is recommended to use the term 'striation-free' in those cases where striations can not be detected or where they are not harmful for the specific application. An absolute striation-free crystal may neither be achieved nor proven, although in facetted growth or in liquid-phase epitaxy in the Frank–Van Der Merwe growth mode quasi striation-free crystals and layers could be expected when step-bunching is prevented.

Various definitions for striations had been suggested. In the following 'functional terms' are proposed that relate to the origin of the specific striations (instead of type-I, type-II, etc.). Striations are defined as growth-induced inhomogeneities in the crystal that are aligned along the facetted or non-facetted growth surface, or in the case of facetted growth with step-bunching are related to the traces of macrosteps.

Table 4.1 Homogeneity requirements of material classes

Crystals, substrates, epilayers	$\Delta X/X$
Semiconductors and solid solutions GaAs/GaP, (Ga,In)As, (Ga,In)Sb, (Cd, Hg)Te	10^{-4} to 10^{-5}
Dielectrics Piezo-electrics, pyroelectrics, electro-optic, Nonlinear-optic and laser crystals	10^{-5} to 10^{-7}
Magnetic and magneto-optic crystals and layers	10^{-4} to 10^{-5}
Metals and alloys	10^{-2} to 10^{-3}

These, often periodic, inhomogeneities are caused in the first case by growth rates which fluctuate with time due to temperature fluctuations and are schematically shown in Figure 4.1(a). Therefore they could be named 'thermal striations'. In Czochralski crystal pulling these striations are frequently linked to crystal rotation rate, since the crystal feels any unsymmetry in the heater-insulation configuration (Camp 1954): these specific thermal striations are called 'rotational striations' or in short 'rotationals'. It was shown by Witt *et al.* (1973) by using time markers and etching of crystal cross sections, that remelting may occur followed by fast growth, so that they defined microscopic (instantaneous) and macroscopic (average) growth rates and thus could explain complex striation patterns. The fluctuating temperatures at the growth interface, leading to growth-rate fluctuations in Czochralski growth, are related to convective instabilities (Hurle 1967), to interactions of several different kinds of flows, which will be discussed further below.

The second class of striations is caused by lateral growth-rate differences as shown in Figure 4.1(b) and are named 'macrostep-induced striations' or 'kinetic striations'. Facetted growth may be observed in growth from melts in small temperature gradients, and it is practically always observed in growth from solutions and from high-temperature solutions. At high densities of growth steps, i.e. at high supersaturation respectively growth rates, the bunching of steps occurs and leads to macrosteps with a large integer of the height of the monostep. For a qualitative explanation of this phenomenon Frank (1958) and Cabrera and Vermilyea (1958) applied the kinematic wave theory that was developed by Lighthill and

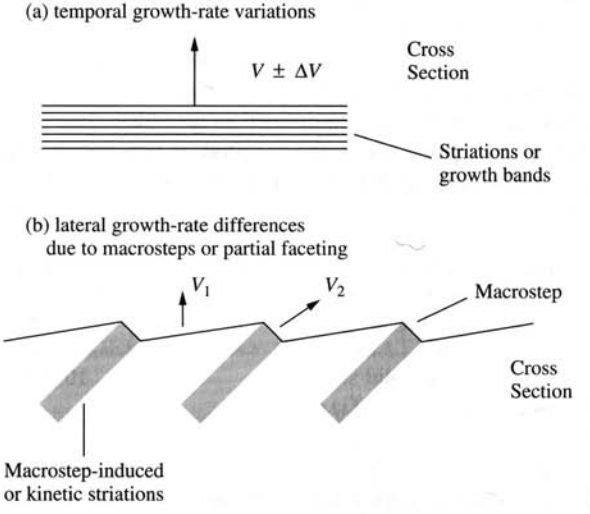

Figure 4.1 Definition of striations (a) caused by temporal growth-rate and temperature fluctuations as 'thermal striations', (b) caused by macrosteps and lateral growth-rate differences as 'macrostep-induced striations' or as 'kinetic striations'.

Whitham (1955) for the general traffic-flow problem. As shown in Figure 4.1(b) growth surfaces with macrosteps respectively with a terrace-and-riser structure with different local growth mechanisms and growth rates: The terrace grows due to lateral propagation of single or double steps with the facet growth rate v_1, whereas the macrostep has the velocity v_2. These growth-rate differences cause corresponding differences in impurity or dopant incorporation and thus lead to the striations which mark the traces of the macrosteps. These 'macrostep-induced' or 'kinetic striations' are shown in Figure 4.2 with LPE-grown multilayers, where the correspondence of the kinetic striations (visible in the angle-lapped and etched p-GaAs layers) with the marked macrosteps is clearly recognized (Scheel 1980). In that work the transition of the misoriented macrostep-surface to the facet with a continuous step propagation by the Frank–Van Der Merwe growth mode is described, a transition that of course leads to layers with excellent homogeneity, i.e. without striations. Chernov and Scheel (1995) analyzed the conditions for achieving such atomically flat surfaces and extremely homogeneous layers (and crystals), see also the epitaxy review of Scheel in this volume.

Macrosteps can be regarded as a first step towards growth instability and are formed not only at high supersaturation, but also in the presence of certain impurities, and on misoriented surfaces (Chernov 1992). When the thermodynamic driving force is further increased, then the impurity built up in front of

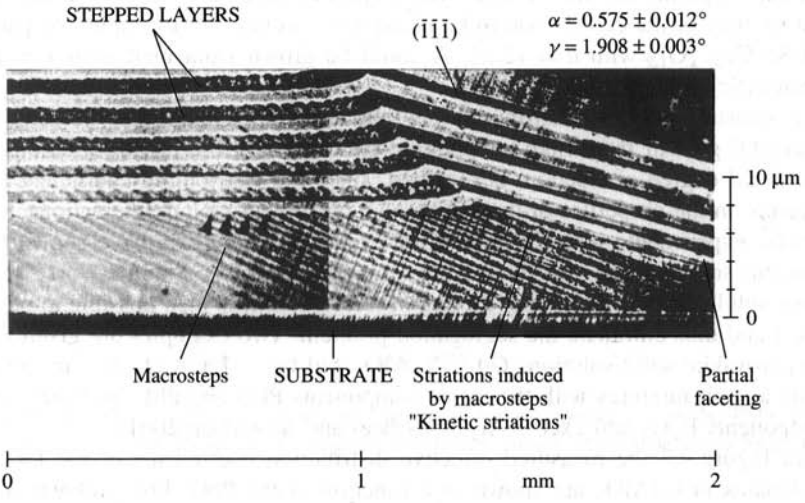

Figure 4.2 Macrostep-induced striations visible in the etched p-GaAs layers of an 11-layer p-/n-GaAs structure grown by liquid phase epitaxy (Scheel 1980). On the GaAs substrate of 0.58° misorientation first a thick layer is grown, which on the right side shows the transition to the {111} facet, whereas the macrostepped surfaces on the left side cause the striations. Angle-lapped ($\gamma = 1.9°$) and etched, composite differential interference (Nomarski) micrograph.

the growing crystal may reach a critical level and is suddenly incorporated, then crystal growth continues until again the impurity is incorporated, and so on. This oscillation of growth rate and impurity incorporation leading to striations was analyzed theoretically and experimentally by Landau (1958). This kind of inhomogeneity could be named 'instability-induced striations'.

4.3 HOMOGENEOUS CRYSTALS WITH $k_{\text{eff}} \rightarrow 1$

The segregation problem is defined by the distribution coefficient k which gives the concentration ratio of a constituent in the grown crystal to that in the growth melt or solution as will be discussed later. Normally k is not unity so that either more constituent is incorporated ($k > 1$) or less constituent than in the growth fluid is built into the crystal ($k < 1$). In these cases $k = 1$ could be achieved in quasi-diffusionless growth, at very high solidification rates. These cannot be applied in bulk crystal growth, but might be acceptable in certain cases of low-dimensional growth, for instance in one-dimensional whiskers or thin rods, or in two-dimensional structures like thin plates or in lateral growth of thin layers.

Mateika (1984) has shown that in the complex garnet structures with tetrahedral, octahedral and dodecahedral sites and by crystal-chemical considerations, cations could be introduced and combined, so that $k = 1$ was achieved. In order to obtain a garnet substrate crystal with a specific lattice constant, the ionic radii and valency of the cations had to be taken into account. For example, the garnet $Gd_3Sc_xGa_{5-x}O_{12}$ with $a = 12.543$ Å could be grown from melt with $x = 1.6$, when $k(\text{Sc}) = 1$.

A constant effective distribution coefficient of unity could also be achieved in crystal growth from high-temperature solutions. By the use of solutions an additional degree of freedom is obtained, since the distribution coefficient also depends on the properties of the solvent and on solvent–solute interactions. Systematic experiments with the growth of oxide solid solutions have shown that different solvents and solvent mixtures may cause $k_{\text{eff}} > 1$ and $k_{\text{eff}} < 1$ for a given solid solution. By proper mixing of the solvent it is then possible to obtain $k = 1$ and thus eliminate the segregation problem. Two examples are given with the perovskite solid solutions $Gd_{1-x}Y_xAlO_3$ and $Gd_{1-x}La_xAlO_3$ that are grown from solvent mixtures with the major components PbO and PbF_2 and the minor components B_2O_3 and excess Al_2O_3 (Scheel and Swendsen 2001).

In Figure 4.3 the measured effective distribution coefficients of the La and Y dopants in $GdAlO_3$ are shown as a function of the PbO–PbF_2 solvent composition. For the pure PbO flux, k_{eff} for La is nearly four, whereas for equal concentrations of oxide and fluoride k_{eff} is less than 0.5. At a composition of about 37 mol% PbF_2, $k_{\text{eff}} = 1$ is obtained. In the case of Y-doped $GdAlO_3$, a nearly pure PbO solvent is required to obtain $k_{\text{eff}} = 1$.

An example of garnet solid solutions grown from PbO–PbF_2 solvent mixtures is shown in Figure 4.4 using the data of Krishnan (1972). Here the distribution

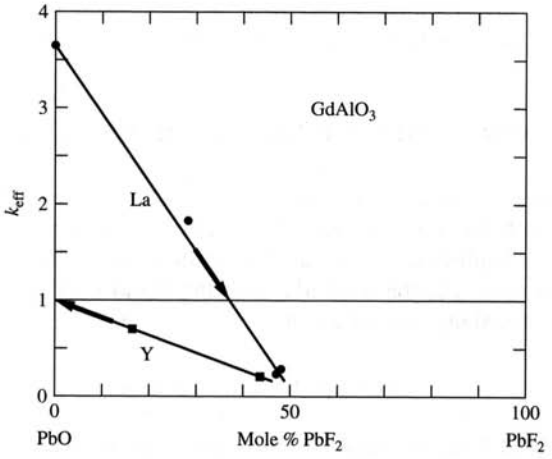

Figure 4.3 The dependence of the effective distribution coefficient on solvent composition in growth of La-doped and Y-doped gadolinium aluminate, after Scheel and Swendsen 2001.

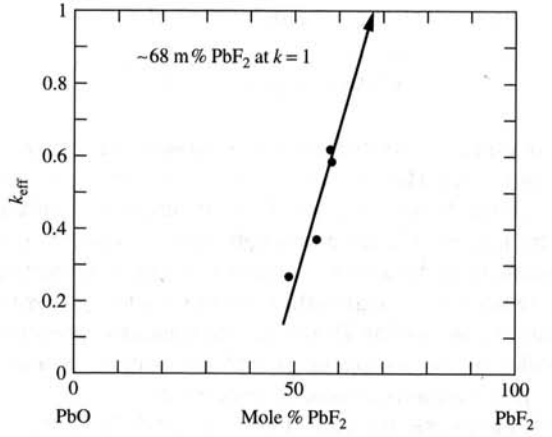

Figure 4.4 The dependence of the effective distribution coefficient on the $PbO-PbF_2$ solvent ratio in flux growth of Cr-doped yttrium iron garnet, after Scheel and Swendsen 2001.

coefficient for Cr in yttrium-iron garnet increases with increasing PbF_2 concentration, so that by extrapolation a solvent mixture with about 32 mol% PbO should give $k_{eff} = 1$. Another example of $Ga_{2-x}Fe_xO_3$ solid solutions grown from PbO-B_2O_3 and Bi_2O_3-B_2O_3 solvent mixtures shows that $k_{eff} = 1$ can be approached with the Bi_2O_3-rich flux (data of Schieber 1966).

A systematic investigation would help to understand these approaches to achieve $k_{\text{eff}} = 1$ and to establish rules for the general applicability.

4.4 SEGREGATION PHENOMENA AND THERMAL STRIATIONS

The concentration of the constituents of a solid solution generally differs from that in the liquid from which the mixed crystal is grown, a phenomenon known as segregation. In equilibrium or at very low growth rates the ratio of the concentration of component A in the solid to that in the liquid is defined as equilibrium segregation (or distribution) coefficient

$$k(\text{A})_0 = C(\text{A})_\text{S}/C(\text{A})_\text{L} \tag{4.1}$$

k_0 may be derived from the equilibrium phase diagram by the ratio of solidus and liquidus concentrations of A at a given temperature.

In a crystallizing system with a limited melt volume, segregation at the growing interface leads to a continuous change of the fluid: $C(\text{A})_\text{L}$ decreases for $k_{\text{eff}} > 1$, and $C(\text{A})_\text{L}$ increases for $k_{\text{eff}} < 1$, so that the concentration $C(\text{A})_\text{S}$ in the solid continuously changes. This causes an inherent concentration gradient in the crystal of which the concentration at any location of the growth front is given by

$$C(\text{A}) = k_{\text{eff}} C_0 (1 - \text{g})^{k_{\text{eff}}^{-1}} \tag{4.2}$$

where g is the fraction of crystallized material and C_0 the initial concentration as derived by Pfann (1952). Here it is assumed that k_{eff} does not vary with concentration or temperature changes. Obviously the inherent concentration gradient can be made zero by keeping the fluid concentration constant. This can be done by growth at constant temperature in combination with transporting feed material from a higher temperature, a growth technique called gradient-transport technique (Elwell and Scheel 1975). However, this approach generally involves large temperature gradients (for acceptable growth rates) and thus leads to temperature fluctuations, so that striations cannot be prevented.

In Figure 4.5 the phase diagram of the system $KTaO_3$–$KNbO_3$ of Reisman *et al.* (1955) is presented where the gradient-transport technique, using the temperature difference T_3 to T_4, is shown. Numerous groups listed by Rytz and Scheel (1982) using this approach could not grow the required striation-free crystals of KTN ($KTa_{1-x}Nb_xO_3$) solid solutions. For electro-optic and other optical applications the variation of x must be smaller than 0.00003, and this requires temperature fluctuations smaller than 0.01 °C as is indicated in Figure 4.5. Also shown is the slow-cooling technique, where a quasiisothermal solution is cooled from T_1 to T_2. This allows to grow striation-free crystals, and the inherent concentration gradient can be kept within tolerated limits by using a large melt. For the KTN system Rytz and Scheel (1982) have calculated the mass of melt M

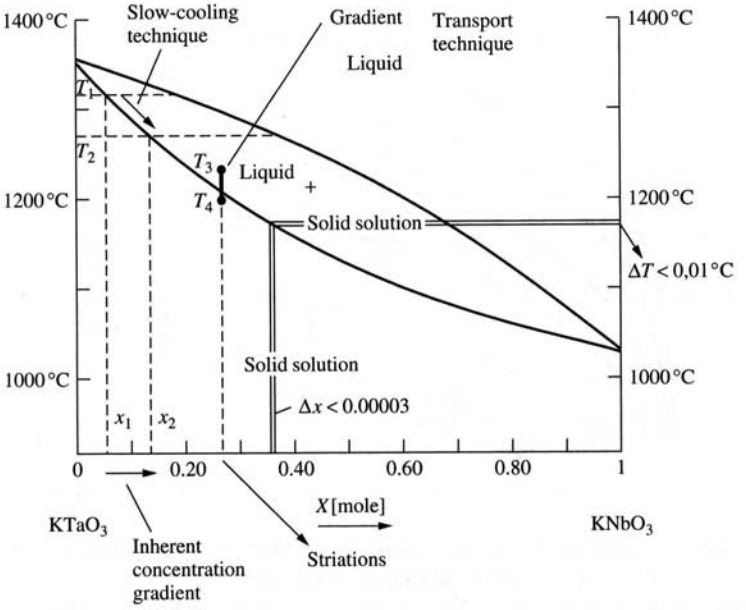

Figure 4.5 The phase diagram $KTaO_3$–$KNbO_3$ of Reisman *et al.* (1955) with indicated growth techniques and resulting inhomogeneities, after Rytz and Scheel 1982.

that is required to grow a crystal of specified volume V with a tolerated inherent concentration difference $x_1 - x_2$. These data and also the temperature cooling range can be read from the nomogram shown in Figure 4.6. For example, a KTN crystal of $1\,cm^3$ with $\Delta x < 0.02$, requires a melt of 1000 g that is cooled by 12 °C. The results of growth experiments will be discussed further below.

In normal crystal growth we have neither the case of very fast growth and $k_{eff} = 1$ nor are we near equilibrium with very low growth rates and $k_{eff} = k_0$, as crystals should be grown at the fastest possible rate that still gives high structural perfection. Figure 4.7 shows the situations at the crystal/liquid interface for the three cases of equilibrium (which theoretically could also be achieved by 'complete' mixing), for the steady-state normal crystal growth, and for fast diffusionless solidification. Also shown are the concentrations in the solid and in the liquid with the diffusion boundary layers. In the steady-state crystal growth the effective distribution coefficient k_{eff} lies between the equilibrium distribution coefficient k_0 and 1 and is dependent on the diffusion boundary layer δ and the growth rate v as shown in Figure 4.7.

For the case of pulling a rotating crystal from the melt by the Czochralski technique, the flow analysis of Cochran (1934) towards an infinite rotating disc was applied by Burton, Prim and Slichter (BPS, 1953a) in order to derive the effective distribution coefficient. Thereby it was considered that the solute concentration

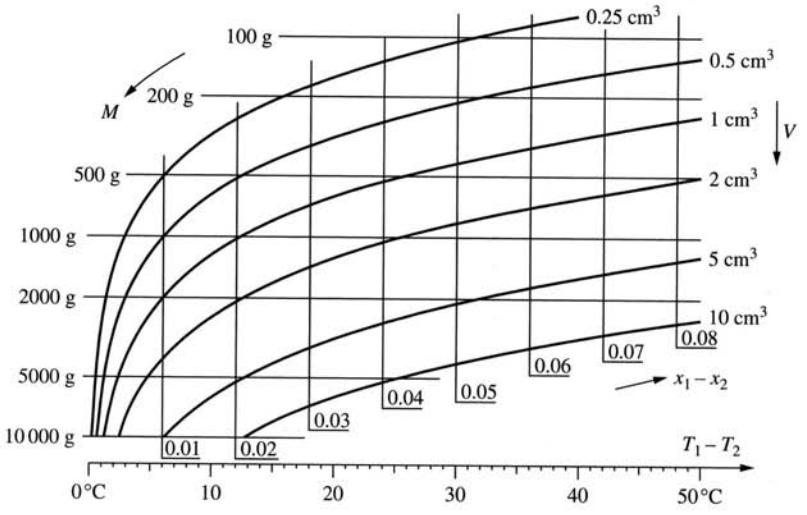

Figure 4.6 Nomogram to read the experimental parameters for growth of KTN solid solution crystals of a specified maximum inhomogeneity $x_1 - x_2$ and volume V. M = mass of the melt, $T_1 - T_2$ is the cooling interval (Rytz and Scheel 1982).

profile is virtually uniform in the radial direction, i.e. the diffusion boundary layer δ can be regarded as having constant thickness across the idealized flat growth interface. Up to a not too large growth rate, δ depends essentially on the crystal rotation rate ω (except for the rim, which is neglected), the kinematic viscosity ν, and a bulk diffusion coefficient D (which includes solute diffusion and solvent counter-diffusion) by

$$\delta = 1.6 D^{1/3} \nu^{1/6} \omega^{1/2}. \tag{4.3}$$

BPS derived for the steady-state case, in which equilibrium prevails at the interface virtually independently of growth rate, the equilibrium distribution coefficient

$$k_{\text{eff}} = k_0 / [k_0 + (1 - k_0) \exp -(v\delta / D)] \tag{4.4}$$

with v the growth rate. In the following, this approximation can be utilized, since the growth-rate dependence of k_0 will be negligible due to the fact that in our attempt to grow striation-free crystals the effective variations of the growth rate are small.

In the accompanying experimental paper Burton *et al.* (1953b) measured the distribution coefficients of several elements in solid/liquid germanium and were able to correlate them with atomic size, respectively, the tetrahedral covalent radii: the larger the element, the smaller the distribution coefficient. They also measured striations by means of incorporated radioactive tracers and photographic

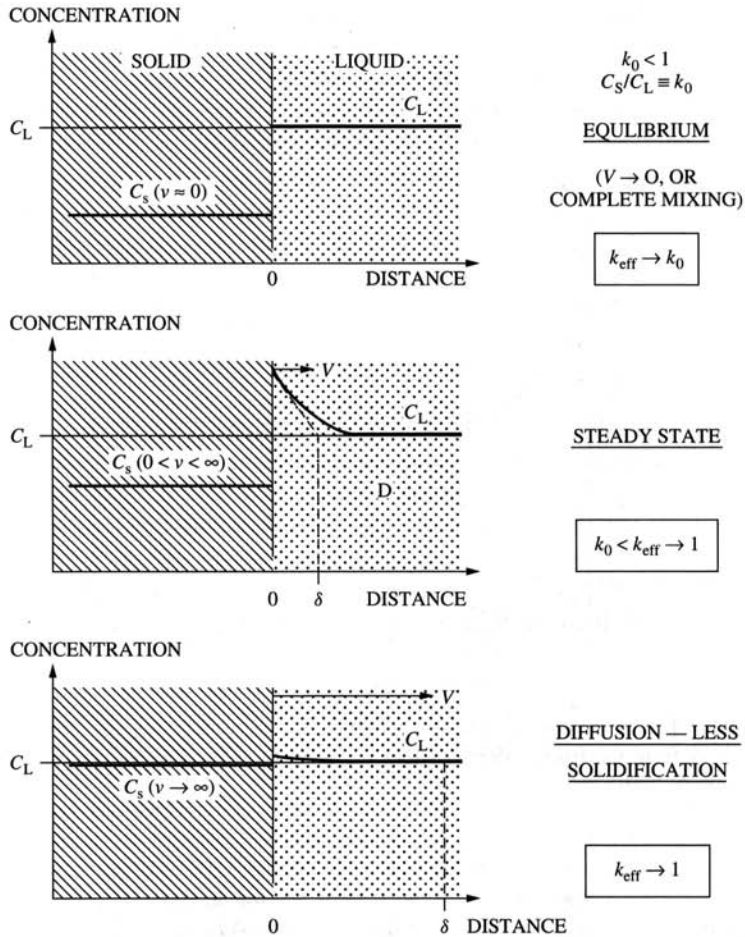

Figure 4.7 The concentration relations at the growth interface and the effective distribution coefficients for three growth situations: near equilibrium k_{eff} approaches k_0, in very fast solidification k_{eff} approaches unity, and in typical crystal growth k_{eff} is between k_0 and 1. The diffusion boundary layer thickness δ depends on the growth rate v and on the flow rate of melt or solution.

film and pointed out the importance of adequate stirring for the growth of homogeneous crystals.

For growth of mixed crystals from dilute solutions, van Erk (1982) has considered the complex solute–solvent interactions and has derived the effective distribution coefficient for diffusion-limited growth as

$$\ln k_{eff} = \ln k_0 - (k_{eff} - 1)(v\delta/D). \tag{4.5}$$

The plotted solutions of Equations (4.4) and (4.5) shown in Figures 4.8 and 4.9, respectively, look similar, but the sensitivity to fluctuations of the growth parameters is different (Scheel and Swendsen 2001).

Growth from solutions is normally limited by volume diffusion, and the relatively fast interface kinetics can be neglected. Based on the diffusion-boundary

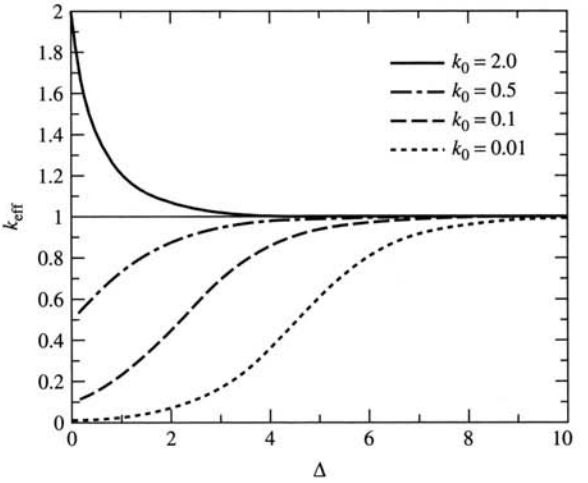

Figure 4.8 The effective distribution coefficient as a function of the exponent $(v\delta/D) = \Delta$ from the Burton-Prim-Slichter Equation (4.4) for four values of k_0 (Scheel and Swendsen 2001).

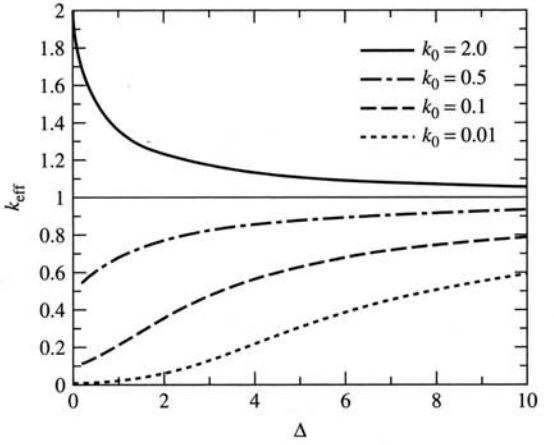

Figure 4.9 The effective distribution coefficient as a function of the exponent Δ from the Van Erk theory and Equation (4.5) for four values of k_0 (Scheel and Swendsen 2001).

layer concept, Nernst (1904) has derived the growth rate as

$$v = D(n_\infty - n_e)/\rho_c\delta \tag{4.6}$$

with n_e and n_∞ the equilibrium and effective bulk concentrations of the solute in the solution, and ρ_c is the solute density. The time constant for the effects of temperature fluctuations (and thus on growth rate v) is on the order of seconds, while that for hydrodynamic fluctuations on δ and v is on the order of minutes. In steady-state growth, within a given range of time and temperature, the diffusion coefficient D and the equilibrium distribution coefficient k_0 in Equations (4.4) and (4.5) can be taken as constants. Therefore the changes in the effective distribution coefficient k_{eff} are essentially determined by the product $(v\delta)$ of the exponent. As a first approximation this product is constant due to the inverse relation between v and δ in the growth-rate Equation (4.6). This means that hydrodynamic changes, which lead to changes of δ, are compensated by growth-rate changes. On the other hand, growth-rate changes caused by temperature fluctuations are not compensated and thus lead to changes of k_{eff} and to thermal striations.

It follows from this discussion that for growth of striation-free crystals the temperature fluctuations should be suppressed to less than about 0.01 °C, and therefore also the temperature gradients should be minimized to less than about 1 °C per cm. On the other hand the crystal has to be cooled to remove the latent heat at practical growth rates, and to control nucleation.

The application of forced convection is recommended for efficient growth. Homogenizing the melts and solutions facilitates the achievement of above temperature conditions, and it reduces the diffusion problems leading to growth instability as discussed in Chapter 6 of Elwell and Scheel (1975). Stirring may be achieved by a continuous flow along the growth interface, by Ekman or Cochran flow towards the rotating growth surface, by periodic flow changes, as in reciprocating stirring in growth from aqueous solutions or by accelerated crucible rotation technique (ACRT) in growth from high-temperature solutions or in growth by the Bridgman–Stockbarger technique, etc.

For many years the favored approach to minimize striations was to reduce convection, to apply microgravity or in the case of semiconductors to apply convection-damping magnetic fields. But the above discussion has shown that, except for special cases requiring large temperature gradients, forced convection has many advantages, not least to achieve economic growth rates approaching the maximum stable growth rates for inclusion-free crystals.

From the above discussion we can also derive the experimental conditions to induce regular striations and superlattice structures, for instance by applying a large temperature gradient in combination with periodic hydrodynamic changes (by ACRT) and applying a constant mean supersaturation, respectively, a constant mean growth rate.

The suppression of striations represents an old problem in crystal-growth technology, and several authors have described striations as an 'inherent', 'intrinsic'

or 'unavoidable' phenomenon in crystal growth, for example Byer (1974), Räuber (1978), and Reiche *et al.* (1980).

In the following, the theoretical considerations discussed above will be applied to an example of growing striation-free crystals of KTN solid solutions which could long not be achieved despite the numerous attempts listed by Rytz and Scheel (1982).

4.5 GROWTH OF STRIATION–FREE KTN CRYSTALS

The solid-solution system $KTa_{1-x}Nb_xO_3$ (KTN) is of interest due to its very large electro-optic coefficient which can be optimized for specific application temperatures by the choice of x (Scheel and Günter 1985). The composition with $x = 0.35$ is used for room-temperature applications, because the ferroelectric transition temperature is then 10 °C and the very large dielectric constant and electro-optic coefficient are observed just above the transition. However, for optical applications the inhomogeneity in refractive index should be less than 10^{-6}, requiring that the crystals and layers be striation-free to this level.

As discussed above, this homogeneity can not be achieved by a gradient-transport technique, but only by slow-cooling of nearly isothermal solutions. The latter was applied by Rytz and Scheel (1982) and Scheel and Sommerauer (1983) who, furthermore, combined an ultra-precise temperature control with optimized temperature distribution in the furnace and applied stirring by the accelerated crucible rotation technique (ACRT) (Scheel 1972) and thus could obtain striation-free KTN crystals for the first time. A typical crucible arrangement with bottom cooling to provide a nucleation site is shown in Figure 4.10 along with the applied ACRT cycle. In ACRT the crucible is periodically accelerated and decelerated so that by inertia the liquid is moving relative to the crucible wall and forms a spiral when seen from top. This spiral shear flow (or spiral shearing distortion) was analyzed and simulated by Schulz-DuBois (1972). He also analyzed the Ekman layer flow in which, under optimized conditions, the liquid is always pumped through a thin Ekman layer at the bottom of the crucible when this is accelerated and decelerated. In Chapter 7 of the book of Elwell and Scheel (1975) the derivation of optimized ACRT stirring based on the kinematic viscosity of the liquid and on the crucible dimension is treated.

Temperature control with a precision of 0.03 °C at around 1300 °C could be achieved by using a thermopile of Pt-6%Rh versus Pt-30%Rh thermocouples (Scheel and West 1973). In Figure 4.11(a) the electromotive forces, i.e. the high-temperature sensitivities of conventional thermocouples and of the 6-fold thermopile are compared whereby the room-temperature sensitivity of the thermopile (Figure 4.11(b)) is practically zero, so that cold-junction compensation is not required. The temperature distribution in the chamber furnace was optimized by arranging heating elements and ceramic insulation according to the reading of numerous thermocouples in the system, and the control thermopile was positioned at the optimum site between heating elements and crucible. KTN crystals

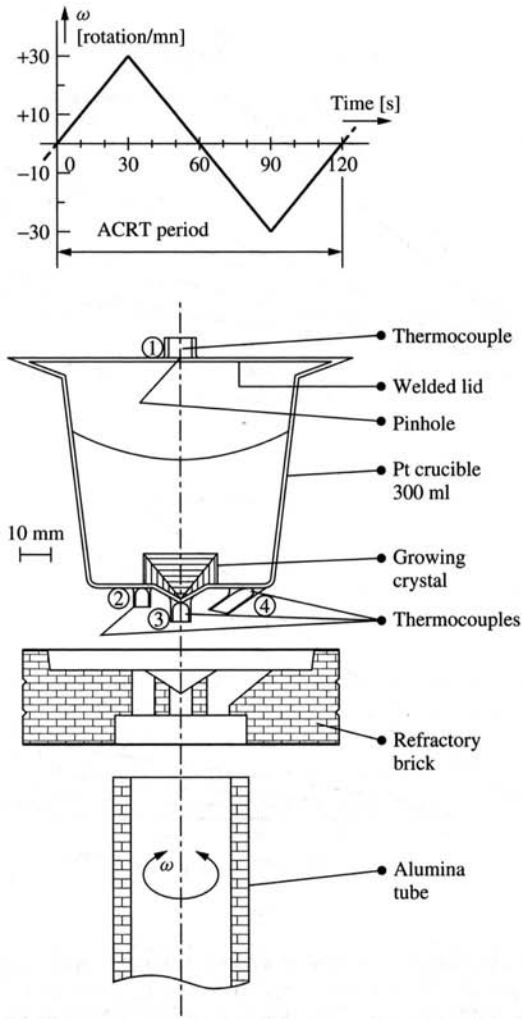

Figure 4.10 Side view of a 300-cm^3 platinum crucible, with welded lid and slightly cooled spot at crucible bottom for nucleation control, used in the ACRT experiments for growth of KTN crystals (Rytz and Scheel 1982). A typical ACRT period is also shown.

with $x = 0.01$ and $x = 0.25$ and up to $33 \times 33 \times 15\,\text{mm}^3$ in size were grown, see Table 4.2 for details of the results.

In the best crystals no striations were visible in a polarizing microscope, although very faint striations could be revealed by using extremely sensitive methods (Scheel and Günter 1985).

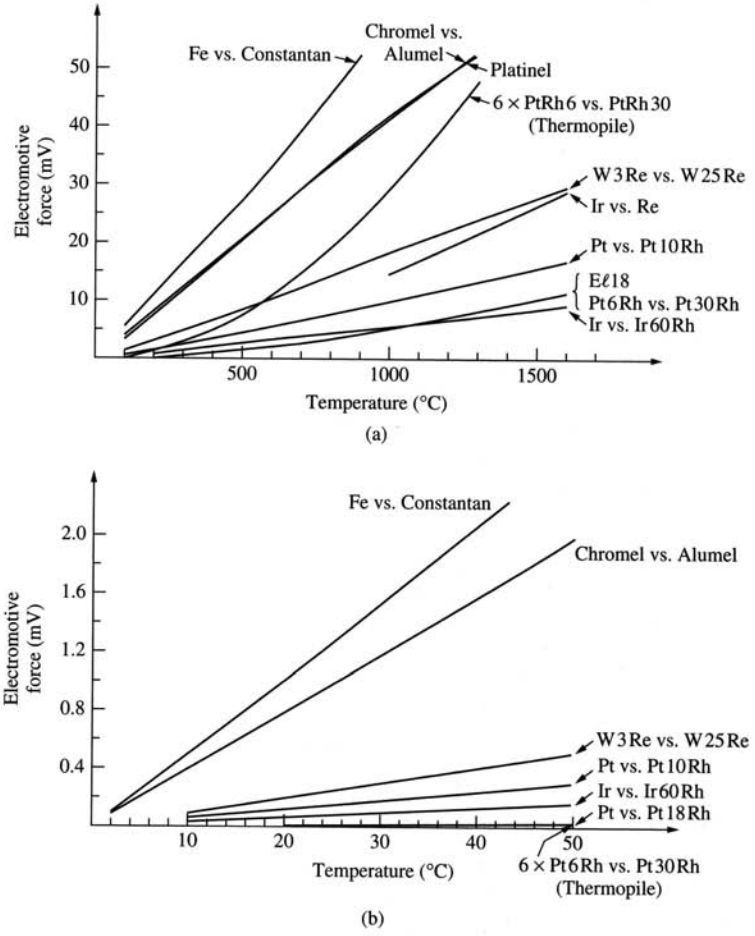

Figure 4.11 The electromotive forces of various common thermocouples (a) for high temperatures, (b) for the temperature range 0 to 50 °C. Note that the thermopile of 6 × PtRh6% versus PtRh30% has a very high sensitivity at high temperatures and practically no sensitivity around room temperature (Scheel and West 1973, from Elwell and Scheel 1975).

4.6 ALTERNATIVE APPROACHES TO REDUCE STRIATIONS

Based on the early studies of striations discussed in Section 4.2, the striations were generally connected with convective oscillations: a clear distinction between the effects of hydrodynamics and of temperature as discussed by Scheel and Swendsen (2001) and in Section 4.4 was not consequently attempted before. This explains the numerous approaches to *reduce* convection in order to solve

Table 4.2 Results of 'striation-free' $KTa_{1-x}Nb_xO_3$ crystals

with $x \sim 0.01$ and $T_c \sim 0\,K$ (Rytz and Scheel 1982) (cooling rate 0.15 °C per hour; ACRT) Crystal size up to $3.5 \times 3.0 \times 1.8\,cm^3$ with 'perfect' regions up to $0.8 \times 0.4 \times 0.4\,cm^3$ $x = 0.0070 \pm 0.00002$ and $\Delta x < 0.0003$/cm (detection limit of ARL electron microprobe and of acoustic resonance measurements) Very faint striations by polarizing microscope, not detectable by electron microprobe
with $x \sim 0.25$ and $T_c \sim 300\,K$ (Scheel and Sommerauer 1983) (cooling rate 0.13 °C per hour; ACRT; growth rate ~500 Å/s) Crystal size up to $3.6 \times 3.3 \times 1.5\,cm^3$ with 'perfect' regions up to $0.5 \times 0.5 \times 0.25\,cm^3$ $\Delta T = 0.1\,°C \sim \Delta x = 0.0003/cm$ at $x = 0.25$ No striations detectable in polarizing microscope and by interferometry (no strain birefringence)
Best literature values for $x \sim 0.25$–0.3: always with striations $\Delta x = 0.006$/cm Fay 1967 $\Delta x = 0.002$/cm Levy and Gashler 1968

the striation problem, whereas it was discussed above that *forced convection* and even *oscillating convection* of quasi-isothermal solutions can solve the striation problem.

In the following, first the attempts to reduce convection will be briefly discussed on the base of the Rayleigh number Ra. At a critical value of Ra one expects the onset of convection in a fluid between a warm bottom plate and a cool top plate (although in reality convection will always occur whenever there is a temperature difference in a real growth system):

$$\mathrm{Ra} = \frac{g\alpha L^3 \Delta T}{k\nu} \tag{4.7}$$

where α is the thermal expansion coefficient, L the fluid height, ΔT the temperature difference, k thermal conductivity, ν the kinematic viscosity, and g the gravitation constant. The first approaches have been to reduce L by means of shallow melts or by baffles below the growth interface in Czochralski crystal pulling. Also double crucibles may have a certain effect on striations (Kozhemyakin 2000), but their greatest advantage is the increased axial crystal yield with the same composition, as it was shown by Benson *et al.* 1981 for silicon and later applied to GaAs and $LiNbO_3$ growth.

Edge-defined film-fed growth EFG allows $k_{eff} \sim 1$ to be approached as was shown theoretically by Kalejs (1978) and experimentally by Fukuda and Hirano (1976) and Matsumura and Fukuda (1976) for platelet growth of doped $LiNbO_3$ and $LiTaO_3$. Shaped growth by pulling downwards has been studied by Miyazawa (1982) who grew relatively homogeneous Te-doped GaSb platelets by 'shaped melt lowering'. A capillary-controlled Czochralski process for shaped crystals

of $Sr_xBa_{1-x}Nb_2O_6$, which has similarity with Stepanov and EFG, was applied by Ivleva *et al.* (1987, 1995) and has led to nearly striation-free crystals due to the thin melt layer between shaping multicapillary die and the crystal. Nakajima (1991) and Kusonoki *et al.* (1991) tried to grow InGaAs solid-solution crystals by ramp-cooling and by GaAs supply at constant temperature similar to W. Bonner, but it seems that large homogeneous crystals for technological use as substrates has not yet been achieved. Ostrogorsky and Müller (1994) proposed a submerged-heater method for vertical Bridgman growth, where the combined effect of thin melt layer and stabilizing temperature gradient should minimize striations, but the complexity has hampered technological application.

Large-scale application has found the modified Czochralski process for pulling huge halide scintillator crystals (up to 700 mm diameter and 550 kg weight) from small melt volumes with liquid feeding by Gektin and Zaslavsky, see in this volume. In this case, there is a combined effect of small liquid volume and forced convection due to counterrotation of crystal and crucible.

But from the time of Skylab and with the available funding for space experiments, the interest shifted in the direction of microgravity, of reduction of g in Equation (4.5). In practical fabrication of semiconductor crystals it was recognized that microgravity would not be applicable for various reasons, so that here the parameter ν of Equation (4.7) was considered: by application of magnetic fields the viscosity was increased, and convection was damped. Magnetic fields were first introduced in 1980 by SONY to silicon production, followed by Fukuda and Terashima, who in 1983 applied magnetic field to GaAs growth, which in industry is still applied in LEC production of specific GaAs products.

Alternative approaches to apply forced convection have been discussed in the Elwell–Scheel book, for instance 'sloshing' of the crucible by moving the center of the container in a horizontal circular path described first by Gunn (1972) as 'sloshing' and later as a special vibration technique by Liu *et al.* (1987). Kirgintsev and Avvakumov (1965) compared various stirring techniques including vibrators and found the latter not very effective. Hayakawa and Kumagawa (1985) and more recently Kozhemyakin (1995) and Zharikov *et al.* revived the interest in vibration stirring, although it has not yet found application in real crystal production.

An optimized technology for growth from solutions using a large rotating seed crystal (or a substrate for liquid phase epitaxy) is shown in Figure 4.12. In bulk growth the grown crystal can be cut off and, after etching to remove the surface damage from slicing, the seed crystal can be used again for the next growth cycle, a little like the large-diameter seed crystals recently developed in silicon Czochralski technology. The optimum crystallographic orientation of the seed is important firstly in view of the growth mechanism to remain at a flat growth surface and to prevent macrostep formation, and secondly with respect to the application of the crystal. In this configuration, a sufficiently high seed rotation rate provides Ekman layer flow and thus a quasiconstant diffusion boundary layer along the crystal surface.

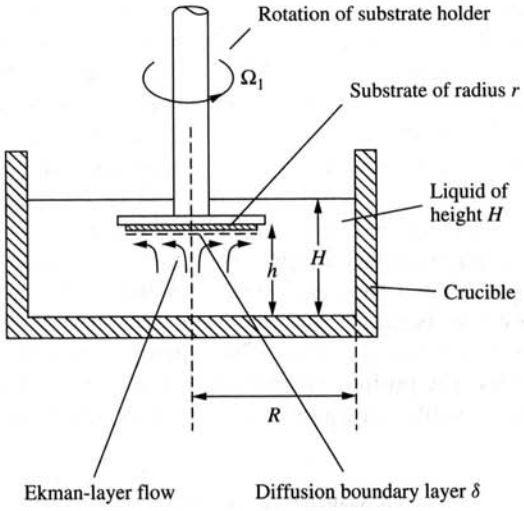

Figure 4.12 An ideal growth system for growth of striation-free large-diameter crystals and of thick and homogeneous LPE layers.

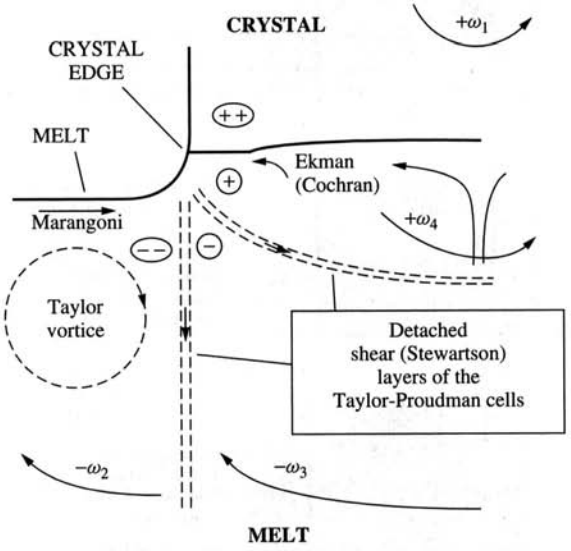

Figure 4.13 More than six types of flow, differing in direction and/or velocity, below the edge of a Czochralski-grown crystal for the case of crystal rotation $+\omega_1$ and crucible counterrotation $-\omega_2$ above the critical Rossby number (Scheel and Sielawa 1985).

For growth from melts by Czochralski crystal pulling there are six or more different kinds of flows below the rim of the crystal as shown in Figure 4.13: flows with different directions and/or different velocities. Double crucibles discussed above will help somewhat to simplify the flow pattern but have practical disadvantages in the growth process. A technologically simpler approach consists of a solid ring coaxial with the crystal rotation axis and rotating with same direction and velocity as the crystal. This ring can be introduced into the melt after complete melting and it can be easily removed at the end of the growth process. In simulation experiments it was shown that at optimized setting of the rotation rate of crystal and ring, and counterrotation of the crucible, the melt fraction inside the ring is nearly stationary and separated from the well-mixed bulk melt, see Figure 4.14. This co-rotating ring Czochralski CRCZ approach of Scheel (1995) has the positive double-crucible effects without the disadvantages of a double crucible: an increased yield of axially homogeneous crystal

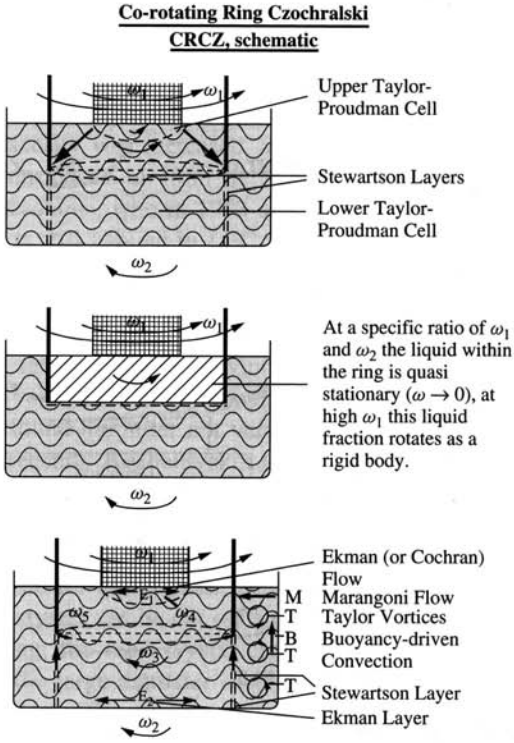

Figure 4.14 Schematic presentation of the Co-rotating ring Czochralski CRCZ concept where the complex flow region of Figure 4.13 is transferred deeper into the melt and where the liquid fraction within the ring can be separated from bulk melt flow under optimized conditions (Scheel 1995).

and reduced striations. Numerical simulations of CRCZ have started (Kakimoto 2002; Zhong Zeng 2001), but the growth technology has yet to be developed.

4.7 DISCUSSION

Several experimental and theoretical solutions were presented to overcome the as intrinsic regarded striation problem:

1. k_0, D, v, δ = constant:	very difficult; chance with rotating seed (Figure 4.12) & with CRCZ (Figure 4.14)
2. k_0, D, v = constant; δ may vary	Rytz & Scheel 1982; Scheel and Sommerauer 1983; Scheel and Swendsen 2001
3. $k_{\text{eff}} = 1$ for growth from melt:	Mateika 1984
4. $k_{\text{eff}} = 1$ for growth from solution:	Scheel and Swendsen 2001
5. Avoid solid solutions by growth of simple stoichiometric compounds with well-defined site distribution from ultra-pure chemicals	

Further conditions are

(a) Continuous flat or smooth growth surface
(b) Isothermal growth surface with $\Delta T/T < 10^{-5}$
(c) Homogeneous melt or solution with $\Delta n/n < 10^{-6}$
(d) Constant growth rate with $\Delta v/v < 10^{-5}$.

These indicated tolerances are typical values and depend on the individual system and on the tolerated inhomogeneity of the crystal. Therefore it is advisable to analyze a new growth system and the phase relations theoretically so that the required technological parameters can be established. With respect to optimized hydrodynamics, simulation experiments with a liquid of similar kinematic viscosity are very useful in the early phase and may be complemented by numerical simulation for process optimization. However, the latter require reliable material (liquid) parameters, which often are not available. In certain cases dimensionless numbers may be helpful to get a feel for the convection regime.

In conclusion, one can say that the striation problem is solvable (on earth) but requires a certain theoretical and technological effort. Hydrodynamic fluctuations are not harmful as long as the fluid is sufficiently isothermal, as long as the transport of fluid of different temperature to the growth interface is suppressed.

REFERENCES

Bardsley W., Boulton J. S. and Hurle D. T. J. (1962), *Solid State Electron.* **5**, 365.
Burton J. A., Prim R. C. and Slichter W. P. (1953a), *J. Chem. Phys.* **21**, 1987.

Burton J. A., Kolb E. D., Slichter W. P., and Struthers J. D. (1953b), *J. Chem. Phys.* **21**, 1991.
Byer R. L. (1974), *Ann. Rev. Mater. Sci.* **4**, 147.
Cabrera N. and Vermilyea D. A. (1958) in *Growth and Perfection of Crystals*, editors R. H. Doremus, B. W. Roberts and D. Turnbull, Wiley, New York and Chapman and Hall, London, p. 393.
Camp P. R. (1954), *J. Appl. Phys.* **25**, 459.
Chen F. S., Geusic J. E., Kurtz S. K., Skinner J. C. and Wemple S. H. (1966), *J. Appl. Phys.* **37**, 388.
Chernov A. A. (1992), *J. Cryst. Growth* **118**, 333.
Chernov A. A. and Scheel H. J. (1995), *J. Cryst. Growth* **149**, 187.
Cockayne B. and Gates M. P. (1967), *J. Mater. Science* **2**, 118.
Donecker J., Lux B. and Reiche P. (1996), *J. Cryst. Growth* **166**, 303.
Elwell D. and Scheel H. J. (1975) *Crystal Growth from High-Temperature Solutions*, Academic Press, London, New York, Chapter 7.
Frank F. C. (1958) in *Growth and Perfection of Crystals*, editors R. H. Doremus, B. W. Roberts and D. Turnbull, Wiley, New York and Chapman and Hall, London, p. 411.
Fukuda T. and Hirano H. (1976), *J. Cryst. Growth* **35**, 127.
Goss A. J., Benson K. E. and Pfann W. G. (1956), *Acta Met.* **4**, 332.
Gunn J. B. (1972), *IBM Tech. Discl. Bull.* **15**, 1050.
Hayakawa Y. and Kumagawa M. (1985), *Cryst. Res. Technol.* **20**, 3.
Hurle D. T. J. (1966), *Philos. Mag.* **13**, 305.
Hurle D. T. J. (1967), in *Crystal Growth*, editor H. S. Peiser, Pergamon, Oxford, 659–663.
Ivleva L. I., Yu. S. Kuz'minov V. V. Osiko and Polozkov N. M. (1987), *J. Cryst. Growth* **82**, 168.
Ivleva L. I., Bogodaev N. V., Polozkov N. M. and Osiko V. V. (1995), *Opt. Mater.* **4**, 168.
Kakimoto K. (2002), private communication.
Kalejs J. P. (1978), *J. Cryst. Growth* **44**, 329.
Kirgintsev A. N. and Avvakumov E. G. (1965), *Sov. Phys.-Cryst.* **10**, 375.
Kozhemyakin G. N. (1995), *J. Cryst. Growth* **149**, 266.
Kozhemyakin G. N. (2000), *J. Cryst. Growth* **220**, 39.
Krishnan R. (1972), *J. Cryst. Growth* **13/14**, 582.
Kusonoki T., Takenaka C. and Nakajima K. (1991), *J. Cryst. Growth* **115**, 723.
Landau A. P. (1958), *Fiz. Metal. Metalloved* **6**, 193.
Laves F. (1944), *Die Chemie* **57**, 30–33; reprinted in *Z. Krist.* **151** (1980) 21.
Lighthill M. J. and Whitham G. B. (1955), *Proc. Roy. Soc.* **229**, 281.
Liu W.-S., Wolf M. F., Elwell D. and Feigelson R. S. (1987) *J. Cryst. Growth* **82**, 589.
Loo R., Kamath G. S. and Knechtli R. C. (1980), *Radiation damage in GaAs solar cells*, 14th IEEE Photovoltaics Specialists Conference.
Mateika D. (1984) in *Current Topics in Materials Science*, editor E. Kaldis, North-Holland/Elsevier, Chapter 2.
Matsumura S. and Fukuda T. (1976), *J. Cryst. Growth* **34**, 350.
Miyazawa S. (1982), *J. Cryst. Growth* **60**, 331.
Nabarro F. R. N. (1975) in *Solution and Precipitation Hardening. The Physics of Metals, Part 2, Defects*, editor P. B. Hirsh, Cambridge University Press Cambridge, p. 152.
Nakajima K. (1991), *J. Cryst. Growth* **110**, 781.
Nernst W. (1904), *Z. Phys. Chem.* **47**, 52.

Ostrogorsky A. G. and G. Müller (1994), *J. Cryst. Growth* **137**, 66.
Pfann W. G. (1952), *J. Met.* **4**, 747.
Räuber A. (1978), in *Current Topics in Materials Science* Vol. 1, editor E. Kaldis, North-Holland, Amsterdam, p. 481.
Reiche P., Schlage R., Bohm J., and Schultze D. (1980), *Kristall U. Technik* **15**, 23.
Reisman A., Triebwasser S. and Holtzberg F. (1955), *J. Am. Chem. Soc.* **77**, 4228.
Rytz D. and Scheel H. J. (1982), *J. Cryst. Growth* **59**, 468.
Scheel H. J. (1972), *J. Cryst. Growth* **13/14**, **560**.
Scheel H. J. (1980), *Appl. Phys. Lett.* **37**, 70.
Scheel H. J. (1995), US Patent 5,471,943.
Scheel H. J. and Günter P. (1985), Chapter 12 in *Crystal Growth of Electronic Materials*, editor E. Kaldis, Elsevier, 149–157.
Scheel H. J. and Sielawa J. T. (1985), Proceedings International Symposium on High-Purity Materials, Dresden/GDR May 6–10, 1985, 232–244.
Scheel H. J. and Sommerauer J. (1983), *J. Cryst. Growth* **62**, 291.
Scheel H. J. and Swendsen R. H. (2001), *J. Cryst. Growth* **233**, 609.
Scheel H. J. and West C. H. (1973), *J. Phys E* **6**, 1178; see also Elwell and Scheel (1975) Chapter 7.
Schieber M. (1966), *J. Appl. Phys.* **37**, 4588.
Schulz-DuBois E. O. (1972), *J. Cryst. Growth* **12**, 81.
Van Erk W. (1982), *J. Cryst. Growth* **57**, 71.
Wenzl H., Oates W. A. and Mika K. (1993), Chapter 3 in *Handbook of Crystal Growth* Vol. 1, editor D. T. J. Hurle, Elsevier, Amsterdam.
Wilcox W. R. and Fullmer L. D. (1965), *J. Appl. Phys.* **36**, 2201.
Zhong Zeng (2001), private communication.